

Four body decay of the lighter top-squark constrained by the Lighter CP-even Higgs boson mass bound

Siba Prasad Das¹

Department of Physics, Jadavpur University, Kolkata- 700 032, India

Abstract

We reinvestigated the parameter space allowing a large BR of the 4-body decay of the lighter top-squark (\tilde{t}_1) accessible at Tevatron Run-II by imposing the lighter CP-even Higgs boson mass (m_{h^0}) bound from LEP. Important constraints were obtained in mSUGRA as well as in the unconstrained supersymmetric models. Our results show that the prospect of searching the lighter top-squark via the 4-body decay mode, in particular the $\ell + n - jets + \cancel{E}_T$ signal, is not promising in mSUGRA due to the above bound on m_{h^0} . The existing bounds on $m_{\tilde{t}_1}$ from Tevatron Run-I and LEP assuming 100% BR of the loop decay of \tilde{t}_1 are, therefore, valid to a good approximation. We also find that large BRs of the above 4-body decay are allowed in the unconstrained model over significant regions of parameter spaces and the possibility that this decay mode is the main discovery channel at Tevatron Run-II is open. We have briefly reviewed the theoretical uncertainties in the calculation of m_{h^0} and their consequences for the constraints obtained by us. We have commented upon, with illustrative examples, how the above parameter space is affected if future experiments push the Higgs boson mass bound upward.

PACS no: 11.30.Pb, 12.60.Jv, 14.80.Ly, 12.60.Fr

¹*spd@juphys.ernet.in*

1 Introduction

The mass of the lighter top-squark (\tilde{t}_1), superpartner of the top-quark in the standard model (SM) may turn out to be below the top-quark mass. This happens in a wide region of the Supersymmetry (SUSY) parameter space both in the minimal Supergravity (mSUGRA) model and in the Minimal Supersymmetric Standard Model (MSSM). It could even be the next-to-lightest supersymmetric particle (NLSP), the lightest neutralino ($\tilde{\chi}_1^0$) being the lightest supersymmetric particle (LSP) by assumption. Being the lightest among the strongly interacting sparticles with a relatively large cross-section compared to other sparticles, the lighter top-squark may show up in direct searches at Tevatron Run-II. In our convention, $\tilde{t}_1 = \tilde{t}_L \cos \theta_{\tilde{t}} + \tilde{t}_R \sin \theta_{\tilde{t}}$ and $\tilde{t}_2 = -\tilde{t}_L \sin \theta_{\tilde{t}} + \tilde{t}_R \cos \theta_{\tilde{t}}$, where $\theta_{\tilde{t}}$ is the mixing angle and \tilde{t}_2 is the heavier top-squark. The top-quark mass (m_t) appears in the off-diagonal elements of the top-squark mass matrix. So, the physical top-squark masses ($m_{\tilde{t}_1}, m_{\tilde{t}_2}$) and the mixing angle depend on the input value of the top-quark mass.

In the lighter top-squark-NLSP (\tilde{t}_1 -NLSP) scenario (*i.e.*, $m_{\tilde{\chi}_1^0} < m_{\tilde{t}_1} <$ the mass of any other sparticle), \tilde{t}_1 has few allowed decay modes in the R-parity conserving (RPC) SUSY model. They are the Flavor Changing Neutral Current (FCNC) induced loop decay, $\tilde{t}_1 \rightarrow c\tilde{\chi}_1^0$ [1], the 4-body decay, $\tilde{t}_1 \rightarrow b\tilde{\chi}_1^0 f\bar{f}'$, where $f\bar{f}' = u, d, c, s, \ell, \nu_\ell$ [2], the tree-level two body decay, $\tilde{t}_1 \rightarrow t\tilde{\chi}_1^0$ and the three body decay, $\tilde{t}_1 \rightarrow bW\tilde{\chi}_1^0$. If $m_{\tilde{t}_1} \gtrsim m_t + m_{\tilde{\chi}_1^0}$, the production cross-section of \tilde{t}_1 is rather low for the Tevatron experiments. The $\tilde{t}_1 \rightarrow bW\tilde{\chi}_1^0$ mode may be suppressed if the coupling $W\tilde{\chi}_1^0\tilde{\chi}_1^\pm$ is small or $m_{\tilde{t}_1} < M_W + m_{\tilde{\chi}_1^0} + m_b$. This may happen if $\tilde{\chi}_1^0$ is bino like as in the mSUGRA model. However, in this report we have considered only those parameter spaces where the last two decay modes are either kinematically or dynamically suppressed.

So far most of the \tilde{t}_1 -NLSP searches at Tevatron Run-I and at the Large Electron Positron (LEP) collider have been performed assuming 100% BR of the loop decay², leading to the signal: jets + missing energy (\cancel{E}_T). The most stringent constraint comes from the Tevatron Run-I experiments [5]. However, the above assumption becomes unrealistic, if \tilde{t}_1 has other decay modes with comparable widths. This possibility exists in a large region of the SUSY parameter spaces in both the models mentioned above [2, 6]. The 4-body decay and the loop decay in RPC models may have decay widths of the same order of magnitude in a wide region of the parameter space [2].

An interesting feature of all supersymmetric models is the prediction of the existence of at least one light Higgs boson [7, 8]. So far the LEP and Tevatron Run-I experiments found no significant evidence in favor of a light Higgs boson. The direct searches from the four LEP experiments concluded that the lighter Higgs boson must be heavier than 114.4 GeV at 95% C.L. [9]. Generally this bound depends on the value of $\sin^2(\beta - \alpha)$, where β and α are the ratio of the vacuum expectation values (VEVs) of the two Higgs doublets and the mixing angle in the CP-even Higgs boson mass matrix respectively. However, the Higgs boson mass

²Recently the $D\bar{0}$ collaboration [3] and the ALEPH collaboration [4] looked for the $\tilde{t}_1 \rightarrow b\tilde{\chi}_1^0 f\bar{f}'$ channel with special assumptions about its BR.

bound is 114.4 GeV when $\sin^2(\beta - \alpha) \simeq 1$. We have found that this factor is indeed $\simeq 1$ for the parameter space interesting for us. This Higgs boson mass bound is directly applicable in SUSY when the CP-odd Higgs boson (M_A) mass is very large compared to Z-boson mass (M_Z), *i.e.*, $M_A \gg M_Z$, commonly known as the decoupling limit.

In SUSY the mass of the light Higgs boson at tree-level is given by,

$$m_{h^0}^2 = \frac{1}{2} \left[M_Z^2 + M_A^2 - \sqrt{(M_Z^2 + M_A^2)^2 - 4M_Z^2 M_A^2 \cos^2 2\beta} \right]. \quad (1)$$

Eqn.1 shows that $m_{h^0} \lesssim M_Z$ at the tree-level. But radiative corrections involving top quark and squarks (\tilde{t}) in the loop indicate that $m_{h^0}^2$ grows like $G_F N_c C m_t^4$ where G_F is the Fermi coupling constant, N_c is the color factor and C is a model dependent loop factor. It is clear that the relatively large experimental error in top mass may lead to a sizable uncertainty in the Higgs boson mass prediction. The loop corrections from bottom quark and squarks (\tilde{b}) are also sizable for large values of $\tan\beta$ and μ [10], where μ is the Higgs mass parameter in the superpotential. We shall discuss the Higgs boson mass as a function of the SUSY model parameters in section 2.

Theoretically the mass of the lighter CP-even Higgs boson is bounded from above: $m_{h^0} \lesssim 135$ GeV. This bound has been obtained by including radiative corrections up to two-loop level [8, 11, 12, 13, 14, 15]. So, m_{h^0} is expected to lie in the range $114.4 \text{ GeV} \lesssim m_{h^0} \lesssim 135 \text{ GeV}$. Due to the yet unknown higher-order corrections the theoretical error on the lighter CP-even Higgs boson mass consists of several pieces [16, 17, 18, 19, 20]. They are the momentum-independent two-loop corrections, the momentum-dependent two-loop corrections, the higher loop corrections from t/\tilde{t} sector etc. Taking into account of all shorts of uncertainties the intrinsic error has been estimated to be $\delta m_{h^0} \approx 3 \text{ GeV}$ ³. However the magnitude of this uncertainty crucially depends on the SUSY parameter space. In view of the above theoretical errors the viability of a parameter space will be judged in this work by using the following two constraints on the calculated Higgs mass: (i) $m_{h^0} \gtrsim 111.4 \text{ GeV}$ (the weaker bound) (ii) $m_{h^0} \gtrsim 114.4 \text{ GeV}$ (the experimental bound). The first bound obviously leads to more conservative results as will be shown in section2.

We now make a few comments on the \tilde{t}_1 decay widths considered in this paper. In the approximation of neglecting the charm quark mass, \tilde{c}_R does not mix with top-squarks. The mixing of \tilde{c}_L with the top-squarks mass eigenstates result in a redefined lighter top-squark given approximately by $\tilde{t}_1 = \tilde{t}_1 + \epsilon \tilde{c}_L$, where

$$\epsilon = \frac{\Delta_L \cos \theta_{\tilde{t}} - \Delta_R \sin \theta_{\tilde{t}}}{m_{\tilde{t}_1}^2 - m_{\tilde{c}_L}^2}. \quad (2)$$

The parameters $\Delta_{L,R}$ are given by

$$\Delta_L = \frac{\alpha}{4\pi s_W^2} \log \left(\frac{M_{\text{GUT}}^2}{M_W^2} \right) \frac{V_{tb}^* V_{cb} m_b^2}{2M_W^2 \cos^2 \beta} \left(m_{\tilde{c}_L}^2 + m_{\tilde{b}_R}^2 + m_{H_d}^2 + A_b^2 \right) \quad (3)$$

³Inclusion of the full two-loop corrections as well as the leading higher loop corrections is expected to yield a reduced uncertainty $\delta m_{h^0} \lesssim 0.5 \text{ GeV}$ [16, 18]

$$\Delta_R = \frac{\alpha}{4\pi s_W^2} \log\left(\frac{M_{\text{GUT}}^2}{M_W^2}\right) \frac{V_{tb}^* V_{cb} m_b^2}{2M_W^2 \cos^2 \beta} m_t A_b, \quad (4)$$

where $m_{\tilde{c}_L}$, $m_{\tilde{b}_R}$, m_{H_d} and A_b are the left-handed scharm, right-handed sbottom, down-type Higgs scalar and trilinear sbottom mass parameters respectively. M_{GUT} is the Grand Unification theory (GUT) scale in SUSY model.

Assuming proper electro-weak symmetry breaking (EWSB), the Higgs scalar mass squared parameter (in Eqn.3) can be written as

$$m_{H_d}^2 = M_A^2 \sin^2 \beta - \cos 2\beta M_W^2 - \mu^2. \quad (5)$$

The loop decay width can then be expressed as [1]:

$$\Gamma(\tilde{t}_1 \rightarrow c\chi_1^0) = \frac{\alpha}{4} m_{\tilde{t}_1} \left(1 - \frac{m_{\chi_1^0}^2}{m_{\tilde{t}_1}^2}\right)^2 |f_{L1}|^2 |\epsilon|^2 \quad (6)$$

where f_{L1} is given by

$$f_{L1} = \sqrt{2} \left[\frac{2}{3}(c_W N_{11} + s_W N_{12}) + \left(\frac{1}{2} - \frac{2}{3} s_W^2\right) \frac{-s_W N_{11} + c_W N_{12}}{c_W s_W} \right] \quad (7)$$

Here N_{11} and N_{12} denote the elements of the neutralino mixing matrix projecting the LSP on to the photino ($j = 1$) and zino ($j = 2$) states. After renormalization one obtains the residual logarithmic terms in Eqns.3 and 4 which lead to a large contribution in the amplitude. Adding various diagrams contributing to the loop, a divergent term is obtained in general. In principle this divergence must be cancelled by adding appropriate counterterms. The dominant effects of renormalization are expected to come from the logarithmic divergences caused by soft breaking terms at M_{GUT} in Supergravity (SUGRA) models. Thus in practice a large logarithmic factor $\ln(M_{\text{GUT}}^2/m_W^2) \sim 65$ is included in the decay amplitude.⁴

The 4-body decay mode $\tilde{t}_1 \rightarrow b\chi_1^0 f f'$, proceeds through various diagrams [2]. An approximate analytical expression for the 4-body decay amplitude can be found in [2]. However, the decay rate has been calculated in [2] without any approximation by taking into account all diagrams and the interferences among them. We thank the authors of [2] for providing their FORTRAN code. The packages SDECAY [21] and CalcHEP v2.1 [22] are now available for calculating the decay width in the context of MSSM. We have cross checked the FORTRAN code with CalcHEP v2.1.

In general, in any diagram the virtuality of the exchanged particle in the propagator is important for getting an appreciable contribution. This gives an idea of the parameter space where the 4-body width is significant. It has been checked that for the \tilde{t}_1 mass range and the

⁴For SUSY breaking mechanisms other than gravity mediation, such as gauge mediation, the SUSY breaking scale can be much lower than the GUT scale, which lead to a somewhat smaller value of Γ in Eqn.6.

model parameters used in this analysis the chargino and/or the slepton mediated diagrams are the dominant ones and the 4-body width is indeed comparable to the loop decay width.

The 4-body and the loop decay of the \tilde{t}_1 -NLSP are of the same order in perturbation theory, i.e. $\mathcal{O}(\alpha^3)$. So, they may compete with each other. Our prime objective is to figure out the SUSY parameter space where the 4-body BR may compete with or overwhelm the loop decay BR. In this perspective a few more points are noteworthy.

- As discussed above the large logarithmic factor in the width (see, Eqns.3 and 4) presupposes the existence of a grand unification scale. Moreover, it is also assumed that MSSM is the correct theory all the way up to M_{GUT} . If this is not the case this factor can be rather small. This would enhance the 4-body BR compared to the typical values presented in this paper.
- If the \tilde{t}_1 is purely right-handed, the amplitude involves only Δ_R in Eqn.2. This will suppress the amplitude for small values of the trilinear coupling A_b (in Eqn.4). Additional suppression may come if the (common) SUSY-breaking scalar mass of the first two generations is large (Eqn.2).
- Any scenario with $\tan\theta_{\tilde{t}} \simeq \Delta_L/\Delta_R$ immediately leads to a negligible ϵ (Eqn.2) .
- From Eqns.3 and 4 we note that the mixing between \tilde{t}_1 and \tilde{c}_L is proportional to $\tan^2\beta$. It is, therefore, relatively suppressed at small $\tan\beta$ which is favourable for a large 4-body BR [2, 6].

It has already been pointed out that the \tilde{t}_1 searches in the 4-body leptonic decay channel is especially promising for $3 \lesssim \tan\beta \lesssim 5$ at the upgraded Tevatron [6]. However, it is also well known that the radiatively corrected m_{h^0} increases with $\tan\beta$. So, what happens to the parameter spaces favourable for \tilde{t}_1 searches in the 4-body decay channel if the Higgs boson mass bound is invoked? We are addressing this issue in this paper.

The input value of top-quark mass in this paper is important for two reasons. Firstly, it changes the parameter space where the \tilde{t}_1 -NLSP condition is satisfied. Consequently the 4-body decay BR will be affected as well for a particular choice of SUSY model parameters. Secondly, as discussed above the, radiative corrections to the Higgs boson mass is very sensitive to m_t .

Before delving into the numerical discussions let us briefly review the current status of the top mass measurement. From the published Tevatron Run-I and preliminary Tevatron Run-II data, the present world average for the top-quark mass is $m_t = 172.7 \pm 2.9$ GeV [23]. Since there is considerable uncertainty in m_t we shall consider in this paper two representative values: (i) $m_t=172.7$ GeV which is the central value of the Run-I and Run-II average and (ii) $m_t=178.0$ GeV which is on the higher side of the currently allowed range (approximately 2σ away from the present central value). The second choice predicts relatively large m_{h^0} for fixed values of other SUSY parameters and hence, leads to weaker constraints on the parameter space allowed by the bound on m_{h^0} .

The plan of the paper is as follows. In section 2, we begin with a discussion of the numerical tools used for calculating the sparticle masses and the lighter CP-even Higgs boson mass. The sub-sections 2.1 and 2.2 are devoted to the phenomenological discussions of the lighter top-squark 4-body decay modes respectively in mSUGRA and MSSM models consistent with the lighter CP-even Higgs boson mass limit from LEP experiments. Consequences of the theoretical uncertainties in the m_{h^0} prediction are also analyzed. We shall conclude in section 3.

2 Numerical Analysis :

We begin with representative parameter spaces in which the \tilde{t}_1 -NLSP condition is realized. We then draw the contours of its total 4-body decay BR in this parameter space. Finally we impose the lighter CP-even Higgs boson mass constraint on this parameter space. The sparticle spectrum in mSUGRA has been calculated using ISAJET v7.48 [24]. The sparticle spectrum in MSSM has been calculated using our own codes. The Higgs boson mass has been calculated using SUSPECT v2.33 [25] in both the models. This code uses the full one-loop and dominant two-loop contributions to the self energy corrections in the SUSY Higgs boson mass matrix in the Dimensional Reduction (\overline{DR}) scheme ⁵.

The supersymmetric radiative corrections to the particle (top, bottom, tau) and sparticles masses (squarks and gauginos) have also been incorporated. We have set the following input values in SUSPECT v2.33 at the weak scale (M_{weak}): $\frac{1}{\alpha_{em}} = \frac{1}{127.934}$, $\alpha_s = 0.1172$, $m_t(\text{pole}) = 172.7$ or 178.0 GeV, $m_\tau(\text{pole}) = 1.777$ GeV, $m_b(m_b) = 4.25$ GeV, $\sin^2_{\theta_W} = 0.2221$.

The M_A and μ are treated as inputs in MSSM in this paper. All masses and mass parameters in this paper are in GeV.

The magnitude of μ can be constrained from the radiative electro-weak symmetry breaking (REWSB) conditions which produce the observed Z-boson mass. Minimizing the Higgs potential with radiative corrections one obtains

$$\frac{1}{2}M_Z^2 = \frac{m_{H_d}^2 - m_{H_u}^2 \tan^2 \beta}{\tan^2 \beta - 1} - \mu^2 + \Delta_R, \quad (8)$$

and

$$\mu B = \frac{1}{2}(m_{H_d}^2 + m_{H_u}^2 + 2\mu^2) \sin 2\beta. \quad (9)$$

, where m_{H_u}, m_{H_d} are the soft Higgs mass parameters at M_{weak} and Δ_R is the radiative correction which is given in [24] and [25]. This REWSB criterion restricts the $|\mu B|$ and $|\mu|$ at M_{weak} and leaves the $sign(\mu)$ as a free parameter in mSUGRA. One can trade the

⁵Other public codes, for example, FeynHiggs [26] and CPsuperH [27] are also available for calculating the properties of the Higgs sector in various SUSY models.

parameter B for $\tan\beta$ (ratio of Higgs VEVs). Eqns.8 and 9 are also valid in MSSM but for arbitrary soft masses.

The soft SUSY breaking terms cannot be arbitrary at M_{weak} in mSUGRA. The soft terms are renormalization group equation (RGE) driven from high scale inputs like the common scalar mass, see sub-section 2.1. The trilinear couplings at M_{weak} can also be computed from a common input value at M_{GUT} using the RGE. The soft terms are treated as independent inputs in MSSM which we shall discuss in the sub-section 2.2 .

However, in both the models one can show that a deep charge-color-breaking (CCB) minima [28, 29, 30] appears in the scalar potential at M_{weak} unless

$$\begin{aligned} |A_t|^2 &\lesssim 3(m_{\tilde{t}_L}^2 + m_{\tilde{t}_R}^2 + m_{H_u}^2 + \mu^2) \\ |A_b|^2 &\lesssim 3(m_{\tilde{b}_L}^2 + m_{\tilde{b}_R}^2 + m_{H_d}^2 + \mu^2) \\ |A_\tau|^2 &\lesssim 3(m_{\tilde{\tau}_L}^2 + m_{\tilde{\tau}_R}^2 + m_{H_d}^2 + \mu^2) \end{aligned} \tag{10}$$

where A_t , A_b and A_τ are the trilinear soft parameters of the top-squark, bottom-squark and tau-slepton sector respectively.

In our analysis we have considered the ranges of model parameters such that the CCB minima [28, 29, 30] of the potential do not arise. Moreover all sparticle masses are required to satisfy the recent experimental bounds. We now make a few comments on the obtained \tilde{t}_1 mass limits.

The published mass limits on \tilde{t}_1 not only depend on the production cross-sections, they also depend on $\Delta M = m_{\tilde{t}_1} - m_{LSP}$, where LSP can be either $\tilde{\chi}_1^0$ or $\tilde{\nu}$. In addition these limits depend on the BRs of various decay channels kinematically allowed. Moreover, the limits from LEP also depend on $\theta_{\tilde{\tau}}$.

Most of the mass limits from Tevatron [31, 32, 33, 34] and LEP [35, 36] have been obtained by assuming 100% BR of the $\tilde{t}_1 \rightarrow c\tilde{\chi}_1^0$ or the $\tilde{t}_1 \rightarrow b\tilde{\chi}_1^+$ decay. However, the presence of other competent decay mode, for example the 4-body decay mode emphasized in this paper, substantially changes these limits. The CDF limit [32] with the above assumption has been included in the analysis of section 2.1.

Recently the DØ collaboration [3] and the ALEPH collaboration [4] put limits on $m_{\tilde{t}_1}$ assuming complete dominance of the channel $\tilde{t}_1 \rightarrow b\tilde{\chi}_1^0\ell\nu_\ell$ and coexistence of the loop decay and the 4-body decay respectively. From Fig.4b of [4] the absolute lower limits of $m_{\tilde{t}_1}$ is found to be ≈ 63 at 95% C.L. . This limit is obtained for $\Delta M = 5$, $BR(\tilde{t}_1 \rightarrow c\tilde{\chi}_1^0)=22\%$ and $BR(\tilde{t}_1 \rightarrow b\tilde{\chi}_1^0\ell\nu_\ell)=55\%$ and $\theta_{\tilde{\tau}}=56^\circ$. The $m_{\tilde{t}_1}$ limit becomes stronger when $BR(\tilde{t}_1 \rightarrow c\tilde{\chi}_1^0)$ is increased from 22%. It may be noted that the assumed BRs in the above works are not realistic. For example it was shown in [6] that the BR of the leptonic ($\ell = e$ and μ) 4-body decay mode is unlikely to exceed 20% since competing hadronic 4-body decay modes are inevitably present. In a different approach [37] model independent limits on the product of branching ratios $BR(\tilde{t}_1 \rightarrow be^+\nu_e\tilde{\chi}_1^0) \times BR(\tilde{t}_1^* \rightarrow \bar{b}q\bar{q}'\tilde{\chi}_1^0)$, where q and q' correspond quarks of all flavours kinematically allowed, were obtained as a function of $m_{\tilde{t}_1}$ using Tevatron Run-I data.

The LEP-II collaboration puts the limit $m_{\tilde{b}_1} \gtrsim 96$ [38] assuming complete dominance of $\tilde{b}_1 \rightarrow b\tilde{\chi}_1^0$ decay. The following constraints on sparticle masses have also been included in the analysis of this paper: $m_{\tilde{\tau}_1} \gtrsim 86$, $m_{\tilde{\nu}} \gtrsim 43.7$, $m_{\tilde{\mu}_R} \gtrsim 94.9$, $m_{\tilde{e}_R} \gtrsim 99.4$ [39] and $m_{\tilde{\chi}_1^\pm} \gtrsim 103$ [40].

2.1 The mSUGRA model:

The input parameters of mSUGRA at M_{GUT} are the common scalar mass (m_0), the common gaugino mass ($m_{1/2}$), the trilinear scalar coupling term (A_0), $\tan\beta$ and sign of μ (the higgsino mass parameter) [41]. The magnitude of μ is fixed by the REWSB condition [28, 42] and depends on the input top quark mass⁶.

Since the NLSP nature of the \tilde{t}_1 is very crucial for our work, we have demarcated different regions in the $A_0 - \tan\beta$ parameter space where \tilde{t}_1 becomes the NLSP. A detailed discussion is given in sec.II of [6] (see Fig.1 and 2⁷ of [6]), where it was assumed that $m_t=175.0$. Similar information is given in Fig.1 and Fig.2 in this paper for $m_t=172.7$ and $m_t=178.0$ respectively. Several contours of the combined BR of all 4-body decay modes are also shown. In order to identify the parameter space allowed by the m_{h^0} constraints, we present the contours of $m_{h^0} \simeq 111.4$ (the weaker bound) in both the figures and $m_{h^0} \simeq 114.4$ (the experimental bound) in the right panel of Fig.2 only.

The choice of other mSUGRA input parameters used are given in the figure captions. These choices are guided by the following facts. If $m_0 \gg m_{1/2}$, the gauginos are naturally light. This disfavors the \tilde{t}_1 -NLSP scenario. For $m_{1/2} \gg m_0$, on the other hand, one may require large $|A_0|$ for this scenario. However, such high values of $|A_0|$ may violate of the CCB conditions, see Eqn.10. So, in our analysis we focused on $m_0 \sim m_{1/2}$ regions for mSUGRA. However, the \tilde{t}_1 -NLSP is quite common in larger regions in the parameter space of the unconstrained MSSM since the soft breaking parameters are arbitrary. This model will be analyzed in the next section.

For each $\tan\beta$ there is a range of $|A_0|$ ($|A_0|_{\text{min}} < |A_0| < |A_0|_{\text{max}}$) at M_{GUT} which corresponds to the \tilde{t}_1 -NLSP (see Fig.1 and 2). Otherwise $\tilde{\tau}_1$ or $\tilde{\chi}_2^0$ or $\tilde{\chi}_1^\pm$ happens to be the NLSP and \tilde{t}_1 decays into other 2-body or 3-body decay channels.

For $|A_0| > |A_0|_{\text{max}}$, \tilde{t}_1 becomes the LSP which is forbidden. On the other hand if $|A_0| < |A_0|_{\text{min}}$ for the given set of mSUGRA parameters, \tilde{t}_1 becomes heavier than the lighter chargino and the \tilde{t}_1 -NLSP condition is violated. We, therefore, concentrate on $|A_0| \sim |A_0|_{\text{min}}$ so that the chargino virtuality is small [2, 6] and consequently the 4-body BR is appreciable. The off-diagonal terms in the top-squark mass matrix have the form $(A_t - \frac{\mu}{\tan\beta})$. So as long as A_t at M_{weak} and μ have opposite signs the NLSP scenario is favored.

For $m_t=172.7$, the \tilde{t}_1 -NLSP is realized in a large region of the parameter space (see Fig.1). As expected the total BR of the 4-body decays is appreciable for relatively low value of $\tan\beta$ [2, 6]. The region above the $m_{h^0} \simeq 111.4$ contour cannot be excluded due to the

⁶The top-quark mass is very crucial for calculating m_{H_u} and Δ_R in Eqns.8 and 9.

⁷One can easily find $m_{\tilde{\chi}_1^0}$ and $m_{\tilde{\chi}_1^\pm}$ from the parameter set used in the figures.

theoretical uncertainties mentioned in the introduction. It should be noted that even with the weaker bound on m_{h^0} the total 4-body decay BR is $\lesssim 5\%$ for $m_0 = 200$, $m_{1/2} = 145$ (see the left panel of Fig.1). For $m_0 = 140$, $m_{1/2} = 180$, on the other hand, the total 4-body decay BR can be as large as 40% (see the right panel of Fig.1). However, the whole parameter space in Fig.1 is disfavoured if the experimental bound is imposed.

A similar analysis for $m_t=178.0$ is shown in Fig.2. In the left panel of Fig.2 with $m_0 = 200$, $m_{1/2} = 145$ we have some allowed region if the weaker bound on m_{h^0} is imposed. Still the total 4-body decay BR can be at most 20%. In the right panel of Fig.2 with $m_0 = 140$, $m_{1/2} = 180$ we have some allowed region even if the experimental bound is imposed. However, the total 4-body decay BR can be at most 20%. Of course with the weaker bound larger 4-body decay BRs ($\lesssim 60\%$) are allowed. It should also be noted that for a fixed m_0 , $m_{1/2}$ cannot be increased arbitrarily because that would lead to other instabilities of the scalar potential [28, 29, 30, 43].

We have shown the variation of $m_{\tilde{t}_1}(m_{h^0})$ as a function of A_0 in the left (right) panel of Fig.3 for $m_t=178.0$ for three values of $\tan\beta$. Other model parameters are given in the figure caption. The \tilde{t}_1 -NLSP criterion is not imposed in this particular figure. However, the range of $m_{\tilde{t}_1}$ satisfying the \tilde{t}_1 -NLSP condition can be easily found out by comparing with the right panel of Fig.2. Then one can read off the lighter chargino and neutralino masses from the left panel of Fig.3. A \tilde{t}_1 having mass in the range shown in Fig.3 may be copiously produced at Tevatron Run-II. From the right panel it is clear that $\tan\beta=5$ is marginally allowed only if the weaker bound on m_{h^0} is required. On the other hand if $\tan\beta \gtrsim 9$ then m_{h^0} is consistent even with the experimental bound, but the total 4-body decay BR is negligible as can be seen from the right panel of Fig.2.

The scatter plots in Fig.4 demarcate the \tilde{t}_1 -NLSP region consistent with the bound on m_{h^0} in the $m_0 - m_{1/2}$ parameter space for positive μ , $m_t=178.0$, $\tan\beta=5$ (left panel) and $\tan\beta=9$ (right panel). In the left panel of Fig.4 with $A_0=-630$ we have some region allowed by the weaker bound on m_{h^0} . The total 4-body decay BR can be as large as 50%. In the right panel of Fig.4 for $\tan\beta=9$ we have some allowed region even after imposing the experimental bound on m_{h^0} but the total 4-body decay BR can be at most 10%. With the weaker bound on m_{h^0} the whole \tilde{t}_1 -NLSP region is allowed. In the regions with $m_{h^0} \simeq 111.4$ the total 4-body BR is $<5\%$.

We have repeated the analysis for $m_t=172.7$ using the same parameters as in Fig.4. In this case the entire \tilde{t}_1 -NLSP region in the $m_0 - m_{1/2}$ parameter space is disfavoured for $\tan\beta=5$ even for the weaker bound on $m_{h^0} \gtrsim 111.4$. For $\tan\beta=9$ on the other hand almost the entire parameter space is allowed by the weaker bound on m_{h^0} . However, the total 4-body BRs can be at most 10% for $\tan\beta=9$.

In [6], we have studied the \tilde{t}_1 search prospects at Tevatron Run-II using the one lepton with 2 or more jets accompanied by a large amount of missing energy signal assuming $m_t=175$. This signal topology arises from the pair production of the lighter top squark followed by the leptonic 4-body decay of one lighter top-squark ($\tilde{t}_1 \rightarrow b\tilde{\chi}_1^0\ell\nu_\ell$) while the other decays hadronically ($\tilde{t}_1 \rightarrow b\tilde{\chi}_1^0q\bar{q}'$). We have shown that, $BR(\tilde{t}_1 \rightarrow b\tilde{\chi}_1^0\ell\nu_\ell) \approx 20\%$, where $\ell = e$ and μ (see Figs.3 and 4 of [6]), is adequate for detection at Tevatron Run-II. From

the present analysis we find that such large leptonic BRs cannot be realized at least in the mSUGRA model for $m_t=172.7$ and not even with the rather conservative choice $m_t=178.0$ irrespective of the m_{h^0} bound invoked. Our analysis also show that the \tilde{t}_1 mass limits from LEP and Tevatron Run-I assuming 100% BR of the loop decay of \tilde{t}_1 are approximately valid in the context of mSUGRA if m_t is close to its current central value (172.7) irrespective of the uncertainties in the predicted m_{h^0} . However, in view of the uncertainties in m_t and in the calculated m_{h^0} one cannot conclusively exclude the possibility of a relatively large total BR of all 4-body decay modes (see, *e.g.*, the right panel of Fig.2).

We have shown some points in the parameter space excluded by the CDF limits on $m_{\tilde{t}_1}$ in Fig.1 (left panel), Fig.2 (left panel) and Fig.4 using the heavy dotted squares. For each of these points $m_{\tilde{\chi}_1^0} \simeq 51$, $m_{\tilde{t}_1} \simeq 102$ and 4-body BR $\simeq 10\%$. It is heartening to note that even the modest statistics from Tevatron Run-I can already put constraints on A_0 which is rather difficult to constrain from other measurements. However, the CDF excluded points are already ruled even by the weaker bound $m_{h^0} \gtrsim 111.4$ in the context of mSUGRA. One notable exception is found in the right panel of Fig.4. Here we find that a small region of parameter space allowed by the weaker bound on m_{h^0} is ruled out by the CDF constraint.

2.2 The MSSM model:

In the MSSM with a universal gaugino mass, the SU(2) gaugino mass parameter (M_2), μ and $\tan\beta$ completely describe the neutralino and chargino masses and mixings. Depending on the relative magnitudes of M_2 and μ , the model is categorized in three different scenarios. They are the higgsino ($M_2 \gg \mu$), the gaugino ($M_2 \ll \mu$) and the mixed ($M_2 \approx \mu$) scenarios. The lighter chargino ($\tilde{\chi}_1^\pm$) and the two lighter neutralinos ($\tilde{\chi}_1^0$ and $\tilde{\chi}_2^0$) all have approximately the same mass ($\approx \mu$) in the higgsino scenario. Thus it is difficult to accommodate the \tilde{t}_1 -NLSP without fine adjustments of the parameters. The \tilde{t}_1 happens to be the NLSP in large regions of the parameter space in the gaugino and the mixed scenarios. In this paper we studied the mixed scenario. However, the main results and conclusions are qualitatively valid in the gaugino scenario.

To calculate $m_{\tilde{t}_1}$ and m_{h^0} in MSSM, we use the parameter X_r (instead of A_0) as input, where

$$X_r = \frac{(A_t - \mu \cot \beta)}{\sqrt{m_{\tilde{u}_L} m_{\tilde{u}_R}}}, \quad (11)$$

$m_{\tilde{u}_L}$ and $m_{\tilde{u}_R}$ are the soft SUSY breaking mass parameters for the first generation left and right-squark respectively at the weak scale.

In our analysis the first generation left and right-squark soft masses are assumed to be the same, *i.e.*, $m_{\tilde{u}_L} = m_{\tilde{u}_R} = m_{\tilde{d}_R} \equiv m_{\tilde{q}}$. The charged slepton sector is also treated similarly, *i.e.*, $m_{\tilde{e}_L} = m_{\tilde{e}_R} \equiv m_{\tilde{l}}$, but the universality of squark and slepton masses is not assumed. These mass patterns can be realized in some variations of the mSUGRA model.

For the third generation squarks the above equality may not hold even in mSUGRA due to, for example, RGE driven by the Yukawa terms. However, the $SU(2)_L$ invariance require

$m_{\tilde{b}_L} = m_{\tilde{t}_L}$ and $m_{\tilde{\nu}_L} = m_{\tilde{\ell}_L}$, neglecting the D-term contributions. In this paper the right and left-squarks soft masses of the third generation are assumed to be equal to $m_{\tilde{q}}$. The physical masses are calculated after incorporating the corresponding fermion masses, the D-terms etc in the mass matrix.

For a given μ , $\tan \beta$, $m_{\tilde{q}}$ and X_r , the trilinear soft breaking mass parameters (A_t) of the top-squark sector can be calculated from Eqn.11. The same parameter for bottom-squark (A_b) and tau-slepton (A_τ) sectors are treated as free input parameters. Using these inputs the third generation squark and slepton masses and mixing angles can be calculated.

We have used the CP-odd Higgs boson mass (M_A) and μ as the free parameters in **SUSPECT v2.33** to calculate the lighter CP-even Higgs boson mass.

The off-diagonal terms in the top-squark mass matrix have the form $m_t X_r m_{\tilde{q}}$. So, the masses and the mixing angle of the top-squark sector are controlled by these parameters. For negative X_r , the $m_{\tilde{t}_1}$ and $m_{\tilde{t}_2}$ are exactly the same as that for positive X_r . The mixing angle depend on the relative magnitude of the diagonal and off-diagonal terms in the top-squark mass matrix.

The $m_{\tilde{t}_1}$ (m_{h^0}) as a function of X_r has been shown for $m_t=172.7$ in the left (right) panel of Fig.5 for four values of $\tan \beta$ (see the figure caption for other input MSSM parameters). $m_{\tilde{t}_1}$ is insensitive to m_t and $\tan \beta$.

The lighter CP-even Higgs boson mass has a periodic dependence on X_r . For a given X_r , if $\tan \beta$ increases the Higgs boson mass also increases. If $\tan \beta=5$ (15) and $m_t=172.7$, $m_{h^0} \simeq 114.4$ for $X_r \simeq 2.0$ (1.5) and $m_{h^0} \simeq 111.4$ for $X_r \simeq 1.75$ (1.30). It is clear from Fig.5 that both the \tilde{t}_1 -NLSP condition and the experimental bound on m_{h^0} may be satisfied for large positive values of X_r . In our subsequent analyses we shall only consider such values of X_r .

Due to the large number of free parameters in MSSM we varied two important parameters at a time keeping the rest fixed.

- $X_r - \tan \beta$

We have demarcated the \tilde{t}_1 -NLSP regions in $X_r - \tan \beta$ plane in the left (right) panel of Fig.6 for $m_t=172.7$ (178.0). Several contours for fixed values of the total BR of 4-body decays are also shown. Comparing with Fig.5 we find that the mass of the \tilde{t}_1 -NLSP is kinematically accessible at Tevatron Run-II. For each $\tan \beta$ there is a range of X_r ($|X_r|_{min} < |X_r| < |X_r|_{max}$) satisfying the \tilde{t}_1 -NLSP condition (recall the A_0 ranges in Figs 1 and 2).

From each BR contour it follows that when X_r is increasing smaller values of $\tan \beta$ are required. For large X_r , $m_{\tilde{t}_1}$ decreases and the virtuality of the exchanged chargino and/or slepton becomes large and tends to suppress the 4-body decay width. In order to keep the BR fixed $\tan \beta$ must be correspondingly reduced.

We have also plotted several contours for $m_{h^0} \simeq 114.4$ and a few other Higgs boson masses. Comparing the left panel of Fig.6 with the right panel of Fig.5 we find that for $m_{h^0} \simeq 111.4$ the \tilde{t}_1 -NLSP condition is violated.

As has already been noted, for $m_t=178.0$ the constraints imposed on the parameter space by the bound on m_{h^0} are less severe (see the right panel of Fig.6). The total 4-body BR can

be as large as 90% for $\tan\beta \simeq 9$ for both choices of m_t in Fig.6. Even a $\tan\beta \simeq 24$ the total 4-body BR is small but not negligible ($\approx 10\%$). In this case it will be interesting to search for hadronic 4-body decays of \tilde{t}_1 at the Large Hadron Collider (LHC) or the International Linear Collider (ILC). Even if $\tan\beta \simeq 3$, $m_{h^0} \simeq 114.4$ is allowed. Consequently almost the entire parameter space in the right panel of Fig.6 is allowed. Such low values of $\tan\beta$ naturally guarantees large total BR of the 4-body decay modes. Moreover we find that the BR of leptonic 4-body decays can be as large as 20%, required for an observable signal at Tevatron Run-II [6].

It is expected that the upcoming collider searches will either discover the Higgs boson or push its mass bound upward. Moreover, the theoretical uncertainties on the Higgs boson mass is likely to be significantly reduced ($\delta m_{h^0} \lesssim 0.5$) [16, 18]. We would now like to comment on the impact of such possible improvements in our understanding of m_{h^0} on \tilde{t}_1 searches. For illustration we have plotted contours of $m_{h^0} \simeq 116.0, 118.0$ and 119.0 ($118.0, 120.0$ and 122.0) for $m_t=172.7$ (178.0) in the left (right) panel of Fig.6. The total 4-body BR $\gtrsim 30\%$ can be completely (nearly) ruled out by an improved Higgs boson mass bound, $m_{h^0} \gtrsim 119.0$ (122.0) if $m_t=172.7$ (178.0) for our choice of other SUSY parameters.

- $X_r - M_A$

We have shown the \tilde{t}_1 -NLSP regions, a few 4-body BR and m_{h^0} contours in the $X_r - M_A$ plane for $m_t=172.7$ and $\tan\beta=5$ (9) in the left (right) panel of Fig.7. The other MSSM model parameters used are mentioned in the figure caption.

The lighter top-squark mass is almost independent of M_A if the other MSSM parameters are fixed. So, the \tilde{t}_1 -NLSP region remains the same when M_A is varied for fixed X_r . The input value of M_A can affect the CCB condition (see Eqns.5, 8 and 10) through the soft breaking Higgs boson masses. This disallows some regions of the parameter space for large X_r . However, the CP-even Higgs boson mass depends on M_A . On the other hand M_A has a nontrivial impact on the loop decay width, see, Eqns.3 and 5 or Ref.[1]. For a fixed X_r if M_A increases the loop decay width also increases. However, the 4-body decay width is insensitive to M_A . So, for large M_A the total 4-body BR decreases for a given X_r . This is very transparent in Fig.7 for relatively large values of X_r corresponding to large virtuality of the exchanged particles in the 4-body decay amplitude.

We find that the total 4-body BR (leptonic BR) can be as large as 90% (20%) in significant regions of the parameter space for $\tan\beta=5$. If the experimental bound on the Higgs boson mass is invoked then the total 4-body BR (leptonic BR) $\simeq 90\%$ (20%) is allowed if $M_A \gtrsim 300$ (400) and $X_r \lesssim 2.17$ (2.08) for $\tan\beta=5$ (see the left panel of Fig.7). We have shown $m_{h^0} \simeq 111.4$ contour in the left panel of Fig.7. It is clear that almost entire parameter space is allowed by the weaker bound on the Higgs boson mass. It has also been checked that the whole \tilde{t}_1 -NLSP region is disfavoured for $m_{h^0} \gtrsim 117.4$.

For $\tan\beta=9$, in the entire \tilde{t}_1 -NLSP region in Fig.7 corresponds to $m_{h^0} \gtrsim 114.4$. However, the total 4-body BR (leptonic BR) $\simeq 90\%$ (20%) occurs only in restricted regions, *i.e.*, $M_A \lesssim 500$ and $X_r \lesssim 2.025$ as can be seen from the right panel of Fig.7.

Since the lower bound on Higgs boson mass may improve in future, we have shown

several m_{h^0} contours, *e.g.* , 115.0 and 115.7 (116.0, 117.0, 117.4, 117.8, 118.4 and 119.0) for $\tan\beta=5$ (9) in the left (right) panel of Fig.7 to illustrate the consequences for the BR under study.

3 Conclusions

The lighter top-squark turns out to be the NLSP in a significant region of the supersymmetric parameter space both in constrained and unconstrained models like mSUGRA and MSSM respectively. The \tilde{t}_1 -NLSP has two competing decay modes for the top-squark masses within the reach of the Tevatron Run-II. They are the loop induced $\tilde{t}_1 \rightarrow c\tilde{\chi}_1^0$ and the 4-body decay, $\tilde{t}_1 \rightarrow b\tilde{\chi}_1^0 f\bar{f}'$. These two decay modes may have comparable decay widths over large regions of parameter spaces in both the models [2, 6]. However, for low $\tan\beta$ the loop decay width is suppressed which in turn enhances the 4-body decay BRs. On the other hand the current bound $m_{h^0} \gtrsim 114.4$ from LEP disfavours low values of $\tan\beta$. It is therefore important to identify the parameter spaces allowing large total BRs of the 4-body decays after imposing the m_{h^0} constraint.

The theoretical uncertainties in the calculated m_{h^0} using any currently available code is ≈ 3 due to the yet unknown higher-order corrections. In view of this we have assumed that realistically the bound on the calculated m_{h^0} can be relaxed to $m_{h^0} \gtrsim 111.4$.

The masses of \tilde{t}_1 and m_{h^0} crucially depend on the input value of m_t . We have considered the current world average central value of m_t which is $m_t=172.7$ as well as $m_t=178.0$, which is approximately 2σ away from the central value and yields somewhat weaker constraints.

We have demarcated the \tilde{t}_1 -NLSP regions in the mSUGRA model for $m_t=172.7$ and 178.0 in the $A_0 - \tan\beta$ (Figs.1 and 2) and $m_0 - m_{1/2}$ planes (Fig.4). We found that for a given $\tan\beta$, a limited range of A_0 with $A_0 \sim |A_0|_{min}$ allows large 4-body BRs. For demonstration we have presented in the $A_0 - \tan\beta$ plane a few 4-body BR contours for two representative choices of m_0 and $m_{1/2}$ (see sub-section 2.1 and the figure captions). For $m_t= 172.7$ all parameter spaces with the total BR of the 4-body decays > 10 (40)% are disfavoured even if the weaker Higgs boson mass bound is invoked (see the left (right) panel of Fig.1). The experimental bound on m_{h^0} rules out any parameter space with numerically significant BR of the above decays. For $m_t= 178.0$ the experimental bound on m_{h^0} leaves no room for total BR > 10 (20)% (see the left (right) panel of Fig.2). The weaker bound, however, allows BRs as large as 30 - 50 % in a small region of the parameter space (the right panel of the above figure).

Complementary information in the $m_0 - m_{1/2}$ plane, for $A_0=-630$, $\text{sign}(\mu) > 0$ and $m_t=178.0$ are presented in Fig.4. For $\tan\beta=5$ the weaker constraint on m_{h^0} allows BRs as large as 60% (see the left panel) in a small parameter space, while the experimental bound on m_{h^0} practically rules out the possibility of a sizable BR of the decay channels of interest. For $\tan\beta = 9$, the total 4-body BR can be at most 10% due to the experimental bound on Higgs boson mass.

We have also excluded small regions in $A_0 - \tan\beta$ and $m_0 - m_{1/2}$ plane from the CDF limits on the mass of \tilde{t}_1 in the jets+ \cancel{E}_T channel. In most cases, however, these constraints are superseded even by the weaker bound on m_{h^0} .

In conclusion we note that in mSUGRA the uncertainties in m_{h^0} and m_t leave open the possibility that the total BR of the 4-body decay of the \tilde{t}_1 -NLSP is sizable although the parameter space corresponding to this scenario is severely squeezed by the bound on m_{h^0} . Perhaps the main future interest in this decay channel in the context of mSUGRA would be to observe it as a rare decay mode at the LHC or the ILC. Moreover, the existing bounds on $m_{\tilde{t}_1}$ obtained by assuming 100% BR of the loop decay are approximately valid in most of the parameter space.

In MSSM we have used the parameter X_r (see Eqn.11) as an input. The interplay of the \tilde{t}_1 -NLSP condition and the Higgs boson mass constraints can be easily followed by varying X_r (see Fig.5). One of the important conclusions is that sizable total BR of the 4-body decays of \tilde{t}_1 can occur for the stronger constraints $m_t = 172.7$, $m_{h^0} \gtrsim 114.4$ and intermediate values of $\tan\beta$ (10 - 15) (see Fig.6). For example, this BR can be as large as 90% in the $X_r - \tan\beta$ plane even for $\tan\beta \approx 9$, $m_{h^0} \gtrsim 114.4$ and $m_t = 172.7$ and 178.0. For lower values of $\tan\beta$ the leptonic 4-body BR $\simeq 20\%$, which can lead to an observable signal at Tevatron Run-II [6], is also consistent with the above constraints. The total BR can be restricted to the level of 10 - 20 % only if the bound on m_{h^0} is significantly improved and m_t is determined with better precision. Complementary information leading to similar conclusions are presented also in the $X_r - M_A$ plane (see Fig.7).

In conclusion we emphasize that the bounds on $m_{\tilde{t}_1}$ from Tevatron obtained by assuming the complete dominance of the loop decay of \tilde{t}_1 requires revision if we want these bounds to be model independent. This is true even though the strong constraint on m_{h^0} from LEP squeezes the parameter space which favours the competing 4-body decays of \tilde{t}_1 . Based on our earlier analyses we conclude that the 4-body mode could still be the main discovery channel for \tilde{t}_1 at both Tevatron Run-II and LHC. As future strategies for the discovering \tilde{t}_1 are planned, attention should be paid to the lighter CP-even Higgs boson search. If its mass bound is significantly improved, the interest in the 4-body decay would be to look for it as a rare decay. It is expected that the Higgs boson may show up at an early stage of LHC the experiments and, at least, some preliminary information on its mass will be available. This information will finally decide the viability of \tilde{t}_1 search in the 4-body decay channel.

Acknowledgement: The author thanks Amitava Datta and Amitava Raychaudhuri for suggestions, comments and careful reading of the manuscript. The author is thankful to M. Guchait, M. Maity and S. Poddar for discussions. A part of the work was supported by the project (SP/S2/K-10/2001) of the Department of Science and Technology (DST), India.

References

- [1] K. Hikasa and M. Kobayashi, Phys. Rev. D **36** (1987) 724 .

- [2] C. Boehm, A. Djouadi and Y. Mambrini, Phys. Rev. D **61** (2000) 095006 .
- [3] DØ Collaboration (V.M. Abazov *et al.*), Phys. Lett. B **581** (2004) 147 .
- [4] ALEPH Collaboration, Phys. Lett. B **537** (2002) 5 .
- [5] For Tevatron Run-I, CDF Collaboration (T. Affolder *et al.*), Phys. Rev. Lett. **88** (2002) 041801 and references therein.
- [6] S. P. Das, A. Datta and M. Guchait, Phys. Rev. D **65** (2002) 095006 .
- [7] J. F. Gunion, H. E. Haber, G. L. Kane and S. Dawson, *The Higgs Hunter's guide*, Addison Wesley, 1990 and (Errata) hep-ph/9302272.
- [8] See *e.g.* , M. Carena and H. E. Haber, Prog. Part. Nucl. Phys. **50** (2003) 63 , hep-ph/0208209.
- [9] See *e.g.* , G. Abbiendi *et al.*, The LEP Working Group for Higgs Boson Searches, Phys. Lett. B **565** (2003) 61 , hep-ex/0306033; also see <http://lepewwg.web.cern.ch/LEPEWWG/>.
- [10] See *e.g.* , S. Heinemeyer, W. Hollik, H. Rzehak and G. Weiglein, Eur. Phys. J. C **39** (2005) 465 .
- [11] S. Heinemeyer, W. Hollik and G. Weiglein, Phys. Rev. D **58** (1998) 091701 , hep-ph/9803277; Phys. Lett. B **440** (1998) 296 , hep-ph/9807423.
- [12] S. Heinemeyer, W. Hollik and G. Weiglein, Eur. Phys. J. C **9** (1999) 343 , hep-ph/9812472.
- [13] J. Casas, J. Espinosa, M. Quirós and A. Riotto, Nucl. Phys. B **436** (1995) 3 , Erratum *ibid.* **439** (1995) 466, hep-ph/9407389.
- [14] M. Carena, J. Espinosa, M. Quirós and C. Wagner, Phys. Lett. B **355** (1995) 209 , hep-ph/9504316; M. Carena, M. Quirós and C. Wagner, Nucl. Phys. B **461** (1996) 407 , hep-ph/9508343.
- [15] H. Haber, R. Hempfling and A. Hoang, Z. Phys. C **75** (1997) 539 , hep-ph/9609331.
- [16] S. Heinemeyer, W. Hollik and G. Weiglein, Phys. Rep. **425** (2006) 265 , hep-ph/0412214.
- [17] S. Heinemeyer, hep-ph/0408340.
- [18] S. Heinemeyer, hep-ph/0407244.
- [19] G. Dedgassi, S. Heinemeyer, W. Hollik, P. Slavich and G. Weiglein, Eur. Phys. J. C **28** (133) 2003 , hep-ph/0212020.

- [20] B. Allanach, A. Djouadi, J. Kneur, W. Porod and P. Slavich, J. High Energy Phys. **0409** (044) 2004 , [hep-ph/0406166](#).
- [21] See *e.g.* , M. Muhlleitner, A. Djouadi and Y. Mambrini, Comp. Phys. Comm. **168** (2005) 46 , [hep-ph/0311167](#).
- [22] See *e.g.* , A.Pukhov, "CalcHEP - a package for evaluation of Feynman diagrams and integration over multi-particle phase-space", see the URL: <http://www.ifh.de/~pukhov/calchep.html>.
- [23] CDF Collaboration, D0 Collaboration and the Tevatron Electroweak Working Group (A. Quadt), [hep-ex/0507091](#).
- [24] See *e.g.* , H. Baer, F.E. Paige, S.D. Protopopescu and X. Tata, [hep-ph/9305342](#) and [hep-ph/0001086](#).
- [25] A. Djouadi, J.L. Kneur and G. Moultaka, [hep-ph/0211331](#).
- [26] S. Heinemeyer, W. Hollik and G. Weiglein, Comp. Phys. Comm. **124** (2000) 76 , [hep-ph/9812320](#); [hep-ph/0002213](#), see <http://www.feynhiggs.de>; M. Frank, S. Heinemeyer, W. Hollik and G. Weiglein, [hep-ph/0202166](#); T. Hahn, S. Heinemeyer, W. Hollik and G. Weiglein, [hep-ph/0507009](#).
- [27] J.S. Lee, A. Pilaftsis, M. Carena, S.Y. Choi, M. Drees, J. Ellis and C.E.M. Wagner, Comp. Phys. Comm. **156** (2004) 283 , [hep-ph/0307377](#).
- [28] L. Alvarez-Gaumé, J. Polchinski and M. Wise, Nucl. Phys. B **221** (1983) 495 .
- [29] See *e.g.* , J.M. Frere, D.R.T. Jones and S. Raby, Nucl. Phys. B **222** (1983) 11 ; M. Claudson, L.J. Hall and I. Hinchliffe, Nucl. Phys. B **228** (1983) 501 ; C. Kounnas *et al.*, Nucl. Phys. B **236** (1984) 438 ; J.P. Derendinger and C.A. Savoy, Nucl. Phys. B **237** (1984) 307 ; M. Drees, M. Glück and K. Grassie, Phys. Lett. B **157** (1985) 164 ; J.F. Gunion, H.E. Haber and M. Sher, Nucl. Phys. B **306** (1988) 1 ; H. Komatsu, Phys. Lett. B **215** (1988) 323 ; J.A. Casas, [hep-ph/9707475](#); M. Brhlik, Nucl. Phys. Proc. Suppl **101** (2001) 395 ; C. Le Mouél, Phys. Rev. D **64** (2001) 075009 and Nucl. Phys. B **607** (2001) 38 .
- [30] J.A. Casas, A. Lleyda and C. Munõz, Nucl. Phys. B **471** (1996) 3 .
- [31] DØ Collaboration (V.M. Abazov *et al.*), Phys. Rev. Lett. **88** (2002) 171802 .
- [32] CDF Collaboration (T. Affolder *et al.*), Phys. Rev. Lett. **84** (2000) 5704 .
- [33] DØ Collaboration, Phys. Rev. Lett. **93** (2004) 011801 .
- [34] CDF Collaboration (T. Affolder *et al.*), Phys. Rev. Lett. **84** (2000) 5273 .

- [35] ALEPH Collaboration (R. Barate *et al.*), Phys. Lett. B **413** (1997) 431 .
- [36] ALEPH Collaboration (R. Barate *et al.*), Phys. Lett. B **488** (2000) 234 .
- [37] S. P. Das, A. Datta and M. Maity, Phys. Lett. B **596** (2004) 293 .
- [38] See *e.g.* , http://lepsusy.web.cern.ch/lepsusy/www/squarks_summer04/stop_combi_208_final.html and the references therein.
- [39] See *e.g.* , http://lepsusy.web.cern.ch/lepsusy/www/sleptons_summer04/slep_final.html and the references therein.
- [40] See *e.g.* , http://lepsusy.web.cern.ch/lepsusy/www/inoslowdmsummer02/chargino_lowdm_pub.html and references therein.
- [41] For a review of mSUGRA and for the physics implications at the Tevatron Run-II, see: S. Abel *et al.*, Report of the SUGRA working group for “Run-II at the Tevatron”, [hep-ph/0003154](http://arxiv.org/abs/hep-ph/0003154) and references therein.
- [42] L. E. Ibanez and G. G. Ross, Phys. Lett. B **110** (1982) 215 ; J. Ellis, D. V. Nanopoulos and K. Tamvaskis, Phys. Lett. B **121** (1983) 123 .
- [43] A. Datta and A. Samanta, Phys. Lett. B **607** (2005) 144 .

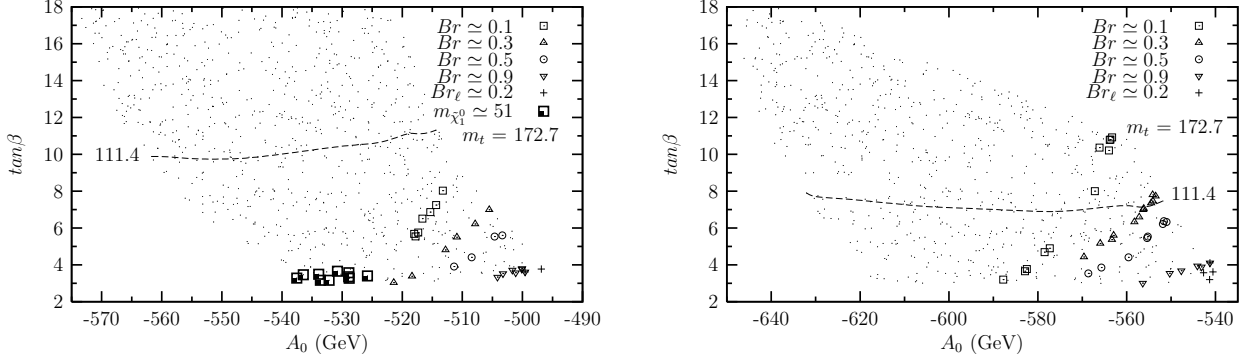


Figure 1: The \tilde{t}_1 becomes the NLSP in the whole marked region in the $A_0 - \tan \beta$ plane in the mSUGRA model for $m_0 = 200(140)$, $m_{1/2} = 145(180)$, $\mu > 0$ and $m_t = 172.7$ in the left (right) panel. The bounds on sparticle masses and other SUSY constraints, see the text, are also imposed. The CP-even Higgs boson mass contour for 111.4 is shown and the region above the contour is allowed (see the text for a brief review of the theoretical uncertainties in the calculated m_{h^0}). The whole marked region is ruled out by the experimental bound $m_{h^0} \gtrsim 114.4$. Several contours of total 4-body decay BR lighter top-squark are shown by different point styles, see the legends. The ‘+’ shows the regions where $BR(\tilde{t}_1 \rightarrow b\tilde{\chi}_1^0 \ell \nu_\ell) \simeq 20\%$ for $\ell=e$ and μ . The regions marked with heavy dotted square box are excluded by the CDF limit ($m_{\tilde{t}_1} \gtrsim 102$ GeV for $m_{\tilde{\chi}_1^0} \approx 51$ GeV) obtained by assuming 100% BR of the loop decay.

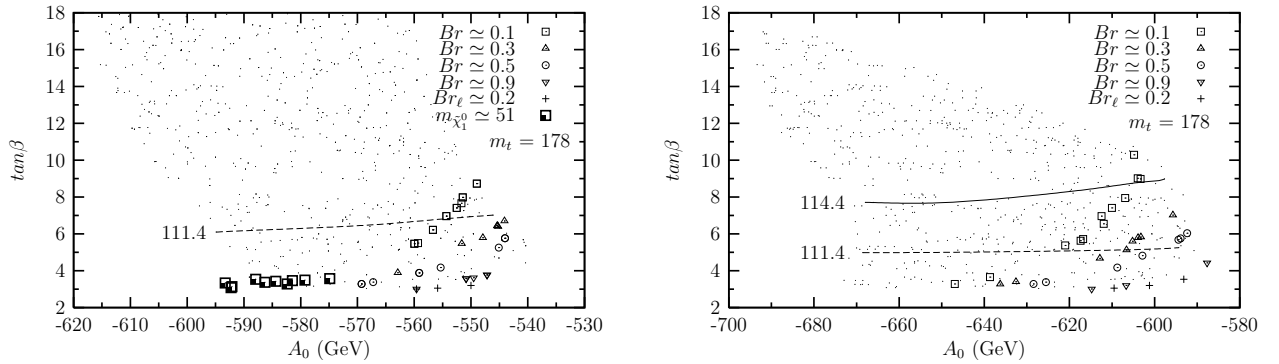


Figure 2: The \tilde{t}_1 becomes the NLSP in the whole marked region in the $A_0 - \tan \beta$ plane in the mSUGRA model for $m_0 = 200(140)$, $m_{1/2} = 145(180)$, $\mu > 0$ and $m_t = 178.0$ in the left (right) panel. The bounds on sparticle masses and other SUSY constraints, see the text, are also imposed. The CP-even Higgs boson mass contours for 111.4 (111.4 and 114.4) are plotted in the left (right) panel and the regions above the contours are allowed from the respective bounds. The whole marked region in the left (right) are ruled out from $m_{h^0} \gtrsim 114.4$ (117.4) (see the text). The total 4-body decay BR's contours of lighter top-squark are shown by different point styles, see the legends. The '+' shows the regions where $BR(\tilde{t}_1 \rightarrow b\tilde{\chi}_1^0 \ell \nu_\ell) \simeq 20\%$ for $\ell=e$ and μ . The regions marked with heavy dotted square box can be excluded by the CDF limit (see Fig.1 caption) .

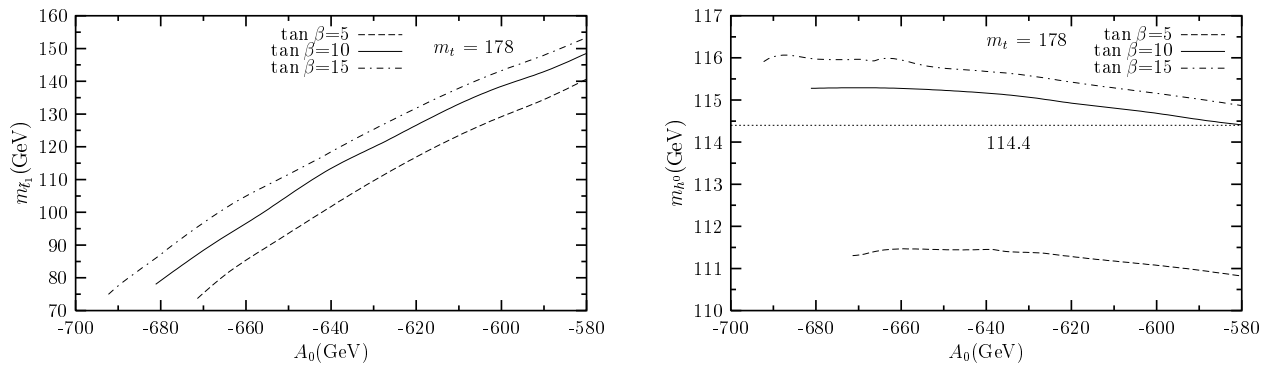


Figure 3: The $m_{\tilde{t}_1}$ (m_{h^0}) as a function of A_0 for $m_0 = 140$, $m_{1/2} = 180$, $\mu > 0$ and $\tan \beta = 5, 10, 15$ in the left (right) panel in mSUGRA for $m_t = 178.0$. The \tilde{t}_1 -NLSP criterion is relaxed in this particular figure.

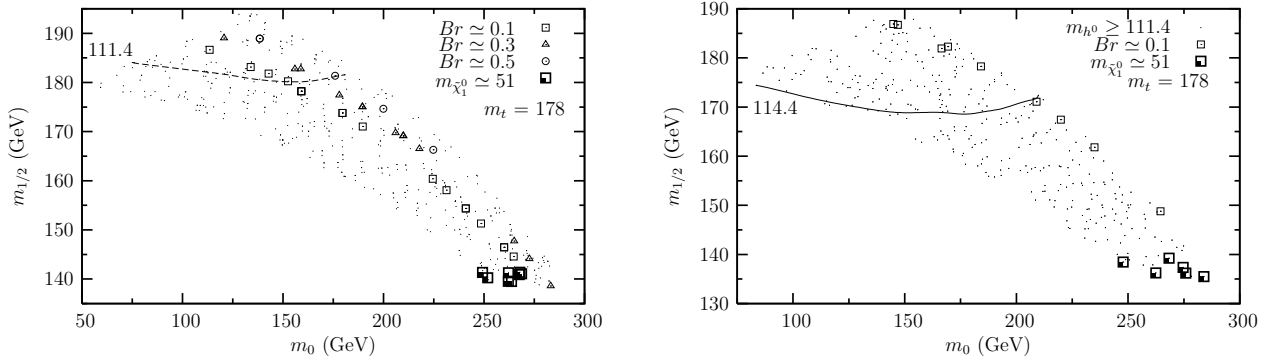


Figure 4: The \tilde{t}_1 becomes the NLSP in the whole marked region in the $m_0 - m_{1/2}$ plane in the mSUGRA model for $A_0 = -630$, $\mu > 0$, $m_t=178.0$ and $\tan\beta =5(9)$ in the left (right) panel. The bounds on sparticle masses and other SUSY constraints, see the text, are also imposed. The CP-even Higgs boson mass contour for 111.4 (114.4) is plotted in the left (right) panel. The m_{h^0} happens to be $\gtrsim 111.4$ in the whole marked region in the right panel. The regions above the contour are allowed from the respective bound on m_{h^0} . The whole marked regions in the left (right) panel are ruled out from $m_{h^0} \gtrsim 114.4$ (117.4). The contours of total 4-body decay BR of the lighter top-squark are shown by different point styles, see the legends. The regions marked with heavy dotted square box can be excluded by the CDF limit (see Fig.1 caption).

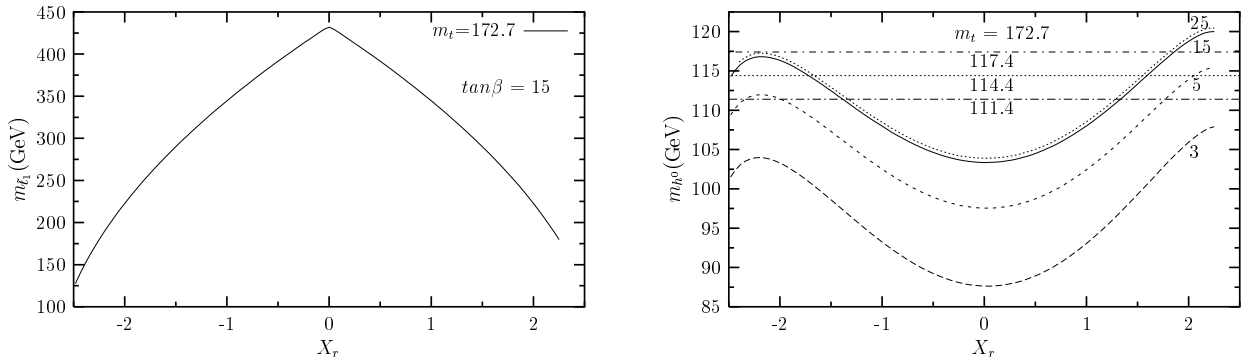


Figure 5: The $m_{\tilde{t}_1}$ (m_{h^0}) as a function of X_r in the MSSM in the left (right) panel for $m_t=172.7$. The MSSM model parameters are: $M_2=300$, $\mu=300$, $M_A=500$, $A_b=200$, $A_\tau=300$, $m_{\tilde{q}} = 400$ and $m_{\tilde{\ell}} = 250$. The choices of $\tan\beta$ are shown in the legends. The \tilde{t}_1 -NLSP criterion is relaxed in this particular figure.

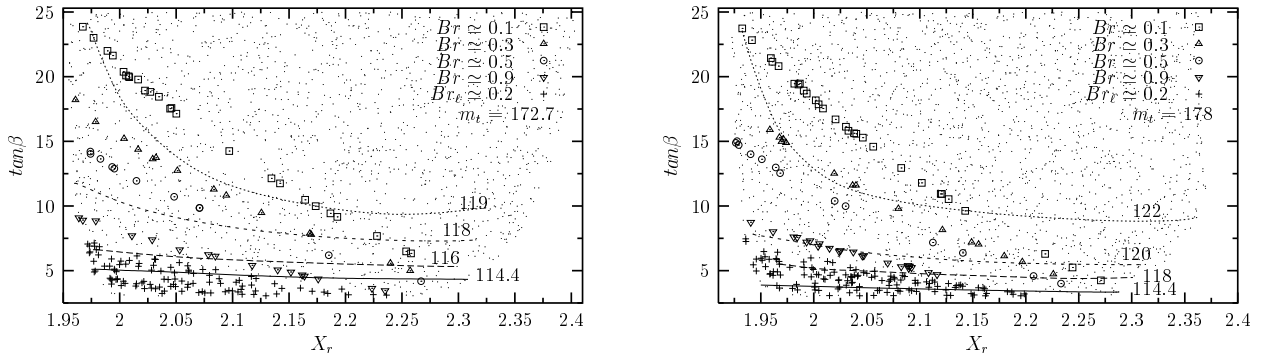


Figure 6: The \tilde{t}_1 is the NLSP in the whole marked region consistent with other sparticle mass bounds in the $X_r - \tan\beta$ plane in the MSSM model for $M_2=300$, $\mu=300$, $M_A=500$, $A_b=200$, $A_\tau=300$, $m_{\tilde{q}} = 400$, $m_{\tilde{\ell}} = 250$ and $m_t = 172.7(178.0)$ in the left (right) panel. The total 4-body decay BRs of the lighter top-squark are shown by the contours with different point styles. The ‘+’ shows the regions where $BR(\tilde{t}_1 \rightarrow b\tilde{\chi}_1^0 \ell \nu_\ell) \simeq 20\%$ for $\ell = e$ and μ . The Higgs boson mass contours for 114.4, 116.0, 118.0 and 119.0 (114.4, 118.0, 120.0 and 122.0) are also plotted in the left (right) panel.

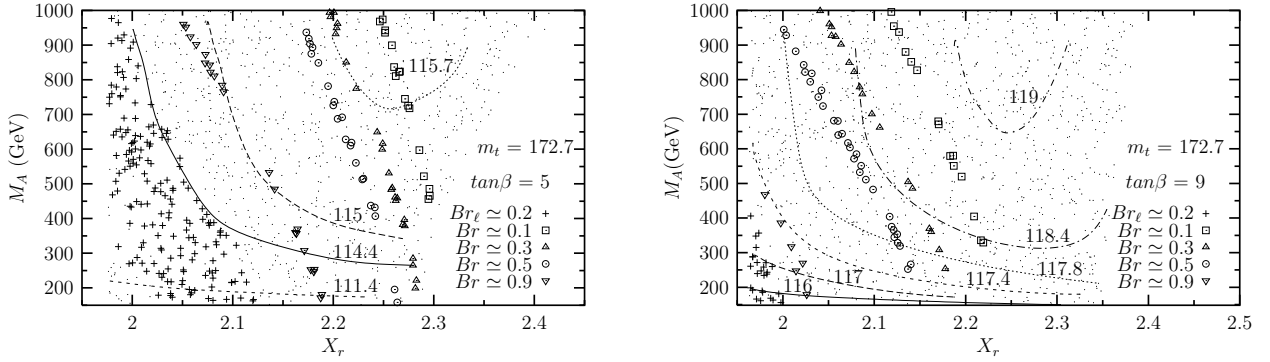


Figure 7: The \tilde{t}_1 is the NLSP in the whole marked region in the $X_r - M_A$ plane in the MSSM model for $M_2 = 300$, $\mu = 300$, $m_{\tilde{q}} = 400$, $m_{\tilde{\ell}} = 250$, $A_b = 200$, $A_\tau = 300$, $m_t = 172.7$ and $\tan\beta = 5(9)$ in the left (right) panel. The total 4-body decay BR of lighter top-squark are shown by different point styles. The ‘+’ shows the regions where $BR(\tilde{t}_1 \rightarrow b\tilde{\chi}_1^0\ell\nu_\ell) \simeq 20\%$ for $\ell = e$ and μ . The Higgs boson mass contours for 111.4, 114.4, 115.0 and 115.7 (116.0, 117.0, 117.4, 117.8, 118.4 and 119.0) are also plotted in the left (right) panel.